

ARTICLE

Received 10 Sep 2012 | Accepted 28 Mar 2013 | Published 30 Apr 2013

DOI: 10.1038/ncomms2820

Non-hyperpolarizing GABA_B receptor activation regulates neuronal migration and neurite growth and specification by cAMP/LKB1

Guillaume Bony¹, Joanna Szczurkowska¹, Ilaria Tamagno¹, Maya Shelly², Andrea Contestabile¹ & Laura Cancedda¹

γ -Aminobutyric acid (GABA) is the principal inhibitory neurotransmitter in adults, acting through ionotropic chloride-permeable GABA_A receptors (GABA_ARs), and metabotropic GABA_BRs coupled to calcium or potassium channels, and cAMP signalling. During early development, GABA is the main neurotransmitter and is not hyperpolarizing, as GABA_AR activation is depolarizing while GABA_BRs lack coupling to potassium channels. Despite extensive knowledge on GABA_ARs as key factors in neuronal development, the role of GABA_BRs remains unclear. Here we address GABA_BR function during rat cortical development by *in utero* knockdown (short interfering RNA) of GABA_BR in pyramidal neuron progenitors. GABA_BR knockdown impairs neuronal migration and axon/dendrite morphological maturation by disrupting cAMP signalling. Furthermore, GABA_BR activation reduces cAMP-dependent phosphorylation of LKB1, a kinase involved in neuronal polarization, and rescues LKB1 overexpression-induced defects in cortical development. Thus, non-hyperpolarizing activation of GABA_BRs during development promotes neuronal migration and morphological maturation by cAMP/LKB1 signalling.

¹Department of Neuroscience and Brain Technologies, Istituto Italiano di Tecnologia, Via Morego, 30 Genoa 16163, Italy. ²Department of Neurobiology and Behavior, State University of New York, Stony Brook, New York 11794 5230, USA. Correspondence and requests for materials should be addressed to L.C. (email: laura.cancedda@iit.it).

γ-Aminobutyric acid (GABA) is the principal inhibitory neurotransmitter in the adult acting through ionotropic GABA_A and metabotropic GABA_B receptors (GABA_ARs, GABA_BRs)^{1,2}. GABA_ARs are chloride-permeable channels. GABA_BRs are heterodimers of GABA_{B1} and GABA_{B2} subunits that operate through G proteins localized at pre- and post-synaptic sites. In particular, GABA_BRs are coupled presynaptically to Ca²⁺ channels, regulating the release of neurotransmitters, and postsynaptically to K⁺ inward rectifying (Kir) channels (Kir3), regulating postsynaptic slow inhibition³. Moreover, GABA_BRs also modulate cyclic AMP (cAMP) signalling, although the physiological consequences of this are poorly understood³. Interestingly, GABA does not mediate hyperpolarization-dependent inhibition during early development, as GABA_AR signalling is mainly depolarizing and excitatory, and GABA_BR lacks coupling between G proteins and Kir3 channels until the end of the first postnatal week^{4,5,6}. Furthermore, abundant endogenous GABA present in neonatal tissue^{1,2,6,7} activates GABA_BRs⁸. Despite the extensive literature on the importance of GABA_AR during early development^{1,2,6,7,9}, the role of GABA_BR has been poorly investigated and data are controversial¹⁰. For example, a role of GABA_BR in neuronal morphological maturation was described in some systems^{9,11,12}, but not in others¹³, and only *in vitro* evidence indicated that GABA_BR modulates migration of immature neurons^{14–17}. Furthermore, these *in vitro* data are in contrast with observations in a number of mouse strains genetically modified for GABA_BRs, which present grossly normal brain and cell morphology^{18–26}. Nevertheless, this may depend on compensatory mechanisms⁶. Here, to investigate GABA_BR function during *in vivo* development, while avoiding compensatory mechanisms, we acutely downregulated GABA_{B2} subunit in a subpopulation of cortical pyramidal-neuron progenitors by *in utero* electroporation. We found that reducing GABA_{B2}-subunit expression results in impairment of cortical migration and morphological maturation of pyramidal neurons, through a mechanism dependent on cAMP signalling.

Results

GABA_{B2} siRNA affects neuronal radial migration *in vivo*. In rodents, glutamatergic neurons are generated in the dorsal ventricular and subventricular zones (VZ, SVZ) of the developing embryonic cortex. After acquisition of a bipolar morphology at the SVZ, these neurons migrate under the guidance of radial glia towards the developing cortical plate (CP), leading to the formation of the layered cortex²⁷. Conversely, interneurons originate at the ganglionic eminence and migrate tangentially to the CP. Interestingly, GABA is more abundant at embryonic stage than at postnatal age^{1,2,6,7}, as we confirmed in interneurons migrating tangentially in the lower intermediate zone (IZ) and in the neuropil (Supplementary Fig. S1a,b). Moreover, GABA_BR is highly expressed at the SVZ and CP (Supplementary Fig. S1c) (ref. 8). To investigate the role of endogenous GABA_BR during development *in vivo*, we used *in utero* electroporation of plasmids encoding small interfering RNA (short interfering RNA, siRNA) to interfere with GABA_B-protein translation in a subpopulation of VZ/SVZ excitatory-neuron progenitors and their neuronal progeny. We prepared three short hairpin RNAs targeting the B₂ subunit of the GABA_BR, and cloned them into the pRNAT-U6.3 expression vector, which drives expression of enhanced green fluorescent protein (EGFP) for visualization of transfected neurons (Supplementary Fig. S2a–c). siRNA1 and siRNA2 efficiently downregulated endogenous GABA_{B2} subunit with siRNA2 exhibiting higher efficiency (Fig. 1a,b; Supplementary Fig. S3a,b). Moreover, whole-cell patch clamp recordings of

GABA_{B2}-induced Kir currents demonstrated that siRNA2 efficiency lasted at least 1 month after electroporation (Fig. 1c,d). siRNac did not produce any effect and was utilized (as the siRNA empty vector) as control (Fig. 1a,b).

First, we examined the functional consequence of GABA_{B2}-subunit downregulation on cortical development by investigating the radial migration of newly generated excitatory cortical neurons. We injected either siRNA1 or siRNA2, or control vectors (siRNA vector or siRNac), into the lateral ventricle of embryonic day 17 (E17) rats *in utero*, and electroporated them into a subpopulation of excitatory-neuron progenitors²⁸. After allowing *in vivo* development, brains at E21, postnatal day 7 (P7), and P16 were cut at the level of the somatosensory cortex. As EGFP expression from the cytomegalovirus promoter in the pRNAT-U6.3 expression vector (Supplementary Fig. S2a–c) decreases with time *in vivo*, siRNA constructs were coelectroporated with pCAG-IRES-tdTomato vector (Tomato, Supplementary Fig. S2f). Tomato vector bears a modified β-actin promoter with a cytomegalovirus immediate-early enhancer expressing a red fluorescence protein (tdTomato) ensuring visualization of transfected cells up to ~1 month (ref. 29). Confocal images of cortical neurons derived from siRNA-transfected progenitors were acquired by using tdTomato fluorescence, which strongly correlated (at E21) with EGFP (siRNA) fluorescence (Pearson product moment correlation, $R = 0.88 \pm 0.05$; $n = 13$ slices, Supplementary Fig. S4a,c) in cells co-transfected *in utero* with siRNA and Tomato vectors (Supplementary Fig. S2b,f).

Four days after electroporation (E21), control siRNA vector/Tomato-labelled cells in coronal slices were found mostly in the CP (Fig. 2a). However, radial migration in siRNA1/Tomato- and siRNA2/Tomato-electroporated animals appeared delayed, as transfected cells were found mostly in the IZ (Fig. 2a). Figure 2b shows a quantification of the number of neurons expressing siRNA1/Tomato or siRNA2/Tomato, or either siRNA vector or siRNac (both included in controls) residing at the VZ, IZ or CP, and normalized to the total number of transfected cells. At P7, control siRNA/Tomato cells all reached cortical layer II/III, whereas a significant percentage of the siRNA1/Tomato and siRNA2/Tomato cells were misplaced (Fig. 2a,c). Similarly, at P16 (as well as at P35) control Tomato cells were all located at cortical layer II/III, whereas a significant percentage of siRNA1/Tomato and siRNA2/Tomato cells remained in deep layers (P16: Fig. 2a,c P35: controls, $0.1 \pm 0.1\%$; siRNA2, $8.1 \pm 1.2\%$). Nevertheless, the general cortical layering seemed preserved, as revealed by immunostaining for the upper-layer neuron-marker Cux1 (red) and nuclear staining with Hoechst (blue, Fig. 2d). Interestingly, we found that ectopic cells with impaired migration showed increased fluorescence-reporter expression (Fig. 2e), which negatively correlated with GABA_{B2} expression in other experiments (Supplementary Fig. S3c). To exclude that the defects in the radial migration may be due to a direct effect of GABA_BR downregulation on radial glia fibres (radial glia is also transfected during *in utero* electroporation), we stained radial glia with specific marker nestin in siRNA vector/Tomato- (control) or siRNA2/Tomato-expressing animals at E21. Nestin immunostaining did not reveal any gross difference in the organization of radial glia scaffold (Supplementary Fig. S5).

Thus, GABA_{B2} downregulation affects the radial migration of excitatory pyramidal neurons *in vivo*, with the strength of this effect depending on the extent of GABA_{B2}-protein downregulation.

GABA_{B2}-siRNA affects axon and dendrite development *in vivo*.

Next, we investigated whether GABA_{B2} downregulation affected morphological maturation of siRNA2-expressing neurons. At

E21, cells electroporated (at E17) with control vectors presented a different morphology depending on their location³⁰. Cells residing at the SVZ, showed a characteristic stellate morphology (Fig. 3a,b) with 4–5 short processes (Fig. 3d). Interestingly, siRNA2/Tomato-transfected cells appeared engulfed in a net of long and thin processes (Fig. 3b,d). On the other hand, control cells at the CP presented the characteristic bipolar morphology of migrating neurons, with a leading process oriented towards the top of the cortex (the future apical dendrite), and a thin trailing process oriented towards the bottom of the cortex (the future axon; Fig. 3a,c). Indeed, transition from multipolar to bipolar morphology determines the polarization of pyramidal neurons, promoting specification of one axon and multiple dendrites. Notably, siRNA2/Tomato neurons had a significantly shorter leading process than controls at the CP (Fig. 3c,e). By P16, migration of control pyramidal neurons was completed and their dendritic trees acquired complex morphology (Fig. 3f,g). However, siRNA2-transfected cells presented short and simple dendritic branching (Fig. 3f,h). Furthermore, ectopic neurons were characterized by a multipolar morphology with long and thin processes (Fig. 3i).

To quantify the effect of siRNA2 on dendritic trees, we performed *post-hoc* reconstructions of layer II/III neurons electroporated *in utero* with control vectors or siRNA2 and filled with biocytin through a patch clamp pipette. GABA_{B2} downregulation significantly reduced apical-dendrite length and branching at P16 (Fig. 4a,b). However, the biocytin-based assay

did not allow analysis of axonal length because long processes were likely cut during acute-slice preparation. Therefore, for axon analyses, we used a GFP fusion protein (see Methods) that localizes at the plasma membrane (mGFP; Supplementary Fig. S2d), which allowed visualization of neurite projections *ex vivo*. Thus, we coelectroporated mGFP and either siRNA vector/Tomato or siRNA2/Tomato in E17 embryos, and analysed axonal development at P16 (Fig. 4c). Quantification of the mGFP fluorescence intensity (normalized to the number of Tomato-positive transfected cells) at the level of dendrites (Fig. 4c, boxed region 1) confirmed impaired dendritic development in siRNA2/Tomato animals (Fig. 4d). Interestingly, we found significantly higher mGFP fluorescence in layer V (axonal intra-cortical projection; Fig. 4c, boxed region 2) and white matter (WM, axonal projections to the contro-lateral cortex; Fig. 4c, boxed region 3), indicating an abnormal expansion of axonal projections in siRNA2/Tomato-transfected neurons of layer II/III (Fig. 4d). Similar results were obtained in animals not only at P7 (dendrites: 37 ± 10% decrease in comparison with controls; axon layer V: 43 ± 9% increase; axon WM: 39 ± 11% increase; Mann–Whitney test, *P* < 0.05), but also at P35 (dendrites: 32 ± 8% decrease in comparison with controls; axon layer V: 49 ± 10% increase; axon WM: 47 ± 13% increase; Mann–Whitney test, *P* < 0.05), indicating that the defect in morphological maturation were not due to a simple delay in developmental growth consequent to hindered migration.

To exclude that siRNA2 transfection affected neuronal development *in vivo* by off-target effects, we generated a complementary DNA encoding a siRNA-resistant GABA_{B2} subunit (mutGABA_{B2}). MutGABA_{B2} bore four silent mutations

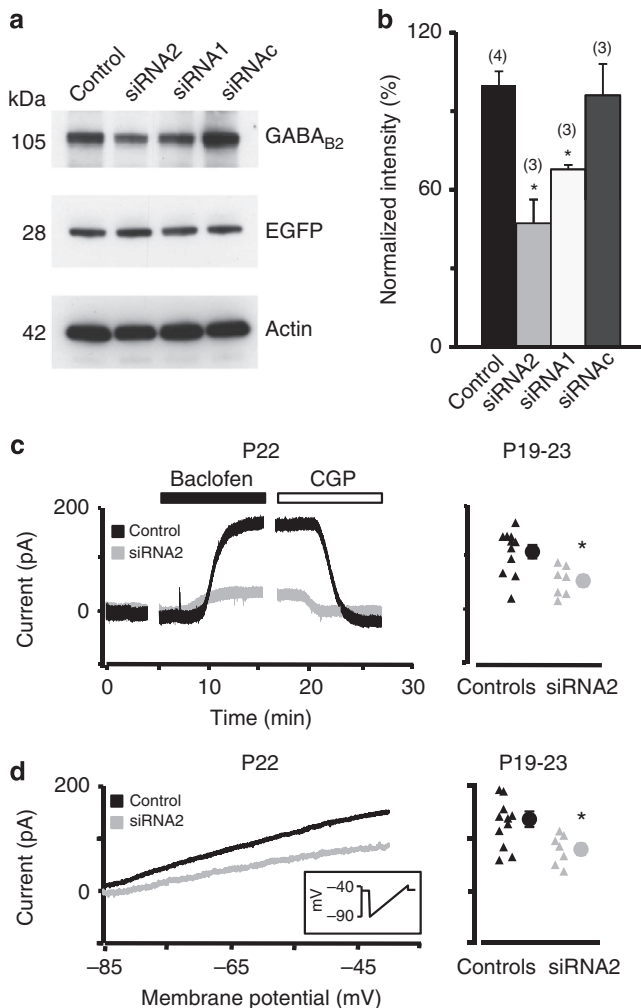


Figure 1 | GABA_{B2}-siRNA allows long-lasting downregulation of endogenous GABA_{B2}-subunit expression. (a) Western blot showing downregulation of GABA_{B2} subunit in cortical neurons in culture at 3 DIV. Three siRNA duplexes (siRNA1, siRNA2 and siRNAC) were tested. Both siRNA1 and siRNA2 were effective in downregulating endogenous GABA_{B2} expression (see Supplementary Fig. S10). (b) Quantification of western blot experiments showing the level of GABA_{B2}-subunit downregulation with the different siRNA duplexes, as in a. Data represent average value normalized to control (siRNA vector) ± s.e.m. The asterisks indicate statistically significant difference compared with control (one-way ANOVA, *P* = 0.003; *post-hoc* Holm–Sidak method, *P* < 0.05). Numbers in parentheses: number of independent transfections. (c) Examples of whole-cell patch clamp recordings of K⁺ currents obtained during bath application of GABA_BR agonist (baclofen, 50 μM) and antagonist (CGP, 2 μM) in acute somatosensory cortical slices from control- (black) and siRNA2- (grey) transfected animals. K⁺ currents were recorded in the presence of TTX (0.1 μM), kynurenic acid (1 mM) and bicuculline (2 μM) to block Na⁺ channels, glutamate ionotropic receptors and GABA_ARs, respectively. Four weeks after *in utero* electroporation, siRNA2-transfected cells were still exhibiting lower K⁺ currents, indicating that siRNA2 was still transcribed and able to downregulate GABA_{B2}-subunit expression. Right: quantification of all recorded K⁺ currents. Triangles represent data from single cells and the circle represents the average ± s.e.m. Data from siRNA2-transfected cells were statistically different (*) from controls (empty vector, WT cells; Student’s *t*-test, *P* = 0.008). (d) Examples of patch clamp recordings of inward rectifying K⁺ currents (reduced current slope at depolarized membrane potentials) during a ramp test protocol (from –90 to –40 mV, 500 ms, inset) in conditions as in c. Peak Kir currents induced by baclofen were calculated as the peak of the trace obtained by the difference of *I*-*V* curves before and after baclofen bath application, as already described²². Right: quantification of the peak amplitude of all recorded currents. Triangles represent data from single cells and the circle represents average ± s.e.m. The asterisk indicates statistically significant difference compared with control (Student’s *t*-test, *P* = 0.016).

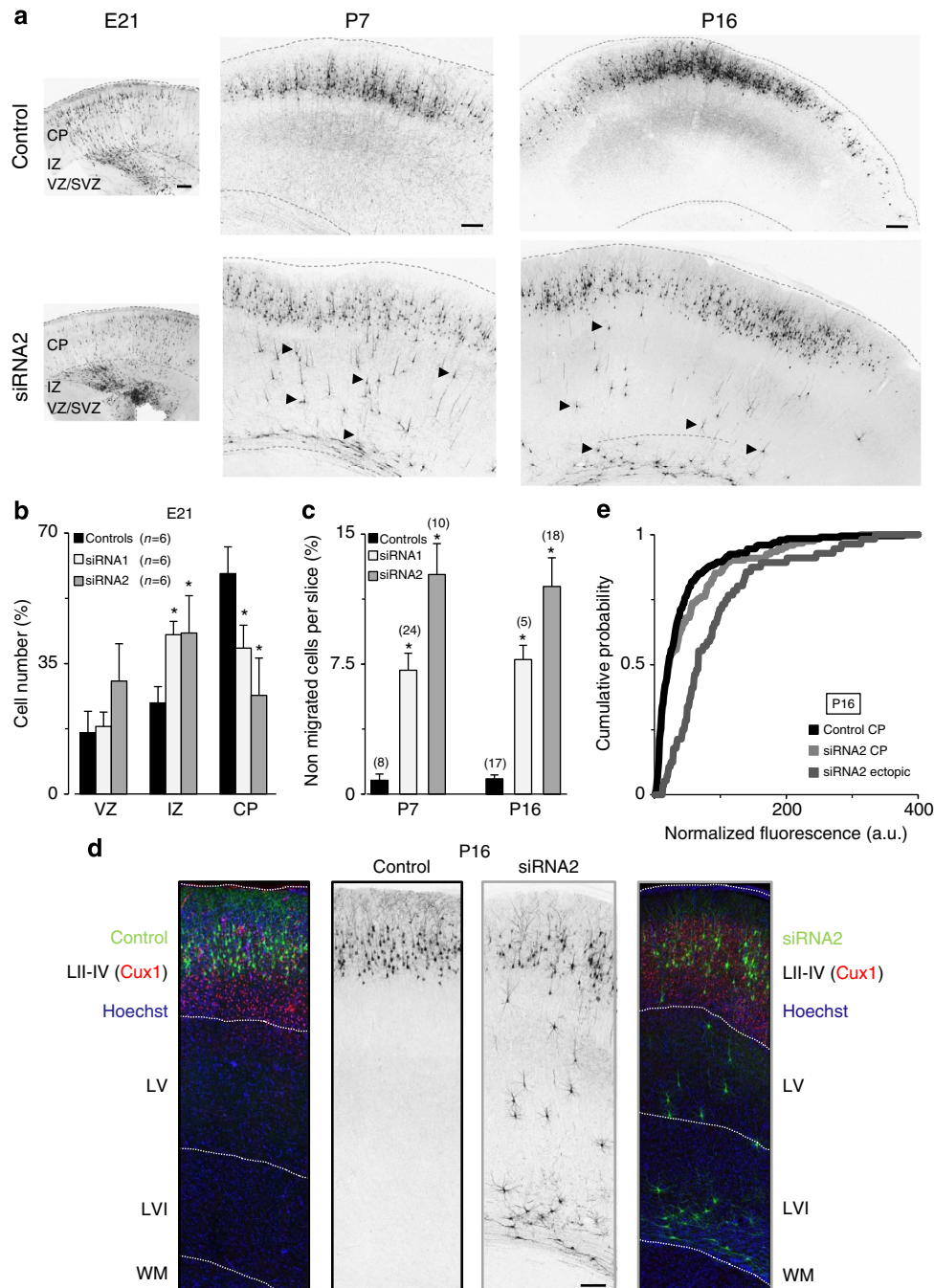


Figure 2 | $GABA_{B2}$ downregulation affects neuronal radial migration *in vivo*. (a) Confocal images of tdTomato fluorescence in coronal sections of rat somatosensory cortices at different ages after *in utero* transfection (at E17) with pRNAT-U6.3 (EGFP) siRNA empty vector together with pCAG-IRES-tdTomato (Tomato, Control), or functional $GABA_{B2}$ -siRNA (siRNA2) together with Tomato construct ($n = 16-64$ animals/experimental age). Arrowheads point to example neurons that did not complete radial migration. Scale bars, 200 μm . (b) Quantification of the number of neurons transfected with either siRNA vector/Tomato or control siRNAc/Tomato (controls, black) or neuron expressing either siRNA1 (light grey) or siRNA2 (dark grey), and residing at the VZ, IZ, or CP (marked by the dotted lines in a) at E21. Numbers are expressed as a percentage of the total number of fluorescent cells in the same section. Asterisks indicate statistically significant difference compared with controls (one-way ANOVA, $P = 0.004$; *post-hoc* Holm-Sidak method, $P < 0.05$). $n =$ number of rats processed (1-3 averaged slices/ per animal). (c) Quantification of the number of control neurons (black) or neurons expressing either siRNA1 (light grey) or siRNA2 (dark grey) that did not complete their migration at different postnatal ages. Asterisks indicate statistically significant difference compared with controls (Kruskal-Wallis one-way ANOVA, $P < 0.001$; *post-hoc* Dunn's method, $P < 0.05$). Numbers in parentheses: number of rats processed (1-3 averaged slices/ per animal). (d) Confocal images of tdTomato fluorescence (green) from empty vector/Tomato- (control) or siRNA2/Tomato-transfected slices stained (at P16) for upper-layer marker Cux1 (red) and nuclear marker Hoechst (blue), showing no defects in general layering of siRNA2-transfected cortices. Dotted white lines delimitate the boundaries of the cortical layers. Scale bar, 150 μm . LII-LIV: layer II-IV; WM: white matter. (e) Cumulative distribution of the average tdTomato-fluorescence intensity at the soma in neurons transfected with control vectors (EGFP/Tomato or siRNA2/Tomato) in the CP (black and light grey, respectively) or with siRNA2/Tomato in ectopic cells (gray) was quantified as a measure of the $GABA_{B2}$ downregulation extent at P16. Ectopic cells exhibited higher tdTomato fluorescence intensity, consistent with severe developmental defects associated with higher levels of siRNA2 expression (Kolmogorov-Smirnov test).

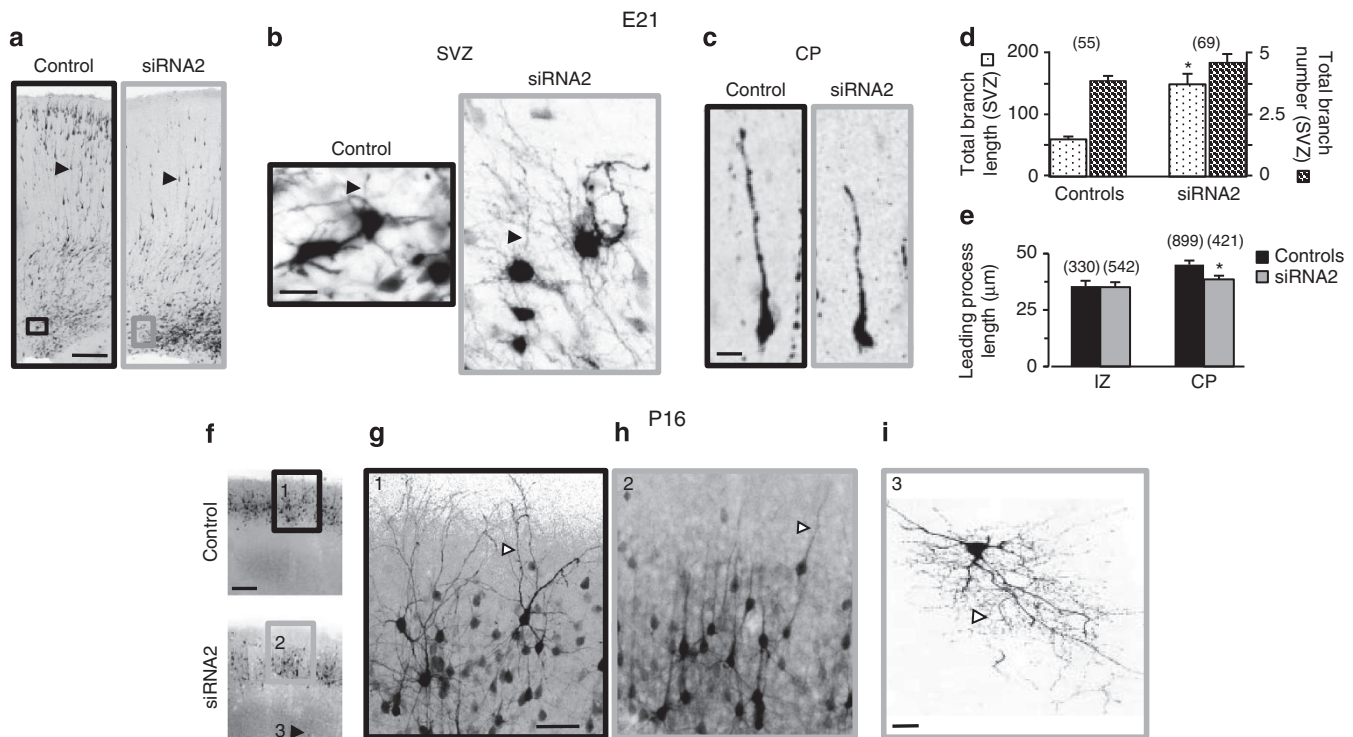


Figure 3 | $GABA_{B2}$ downregulation specifically affects axon/dendrite morphological maturation of pyramidal neurons *in vivo*. (a) Confocal images of tdTomato fluorescence in coronal sections of somatosensory cortices from E21 rats transfected *in utero* with control siRNA vector/Tomato (black) or siRNA2/Tomato (grey) construct. Scale bar, 200 μm . (b) Higher magnifications of SVZ fields from boxed regions as in a. Note the abundance of long and thin processes in siRNA2-transfected cells in comparison with normal stellate morphology of SVZ control neurons (black arrowheads). Scale bar, 25 μm . (c) High-magnification images of typical bipolar migrating neurons from the CP (as indicated by arrowheads in a), showing a longer leading process in control than in $GABA_{B2}$ -downregulated cells. Scale bar, 10 μm . (d) Quantification of the total branch length (dots) and branch number (lines) of neurons expressing either siRNA vector/Tomato or siRNac/Tomato (controls), or siRNA2/Tomato in the SVZ at E21. The asterisk indicates statistically significant difference compared with controls (Mann-Whitney Test, $P < 0.001$). Numbers in parentheses: number of cells processed (control, four rats; siRNA2, six rats). (e) Quantification of the leading process length of control neurons (black), or siRNA2/Tomato (grey) at E21. The asterisk indicates statistically significant difference compared with controls (one-way ANOVA, $P < 0.001$; *post-hoc* Holm-Sidak method, $P < 0.05$). Numbers in parentheses: number of cells processed (control four rats, siRNA2 six rats). (f) Confocal images of tdTomato fluorescence in coronal sections of somatosensory cortices from P16 rats transfected *in utero* with siRNA vector/Tomato (top) or siRNA2/Tomato (bottom) constructs. Scale bar, 300 μm . (g,h) Control neurons showed thick and long apical dendrites, whereas $GABA_{B2}$ downregulation impaired dendritic development (white arrowheads). (i) Thin and long processes (white arrowhead) were observed in ectopic cells located at deep cortical layers (as indicated by the black arrowhead in f) in siRNA2/Tomato-transfected cells. Images (g,h,i) are magnifications from square boxes in f. Scale bars: 100 μm , images 1-2; 25 μm , image 3.

in the siRNA2-target sequence (Fig. 5a), and it was cloned into pCAG-IRES-tdTomato (Supplementary Fig. S2g). Co-transfection of mut $GABA_{B2}$ and siRNA2 in cortical neurons in culture at days *in vitro* 3 (3 DIV) revealed overexpression of $GABA_{B2}$ even in the presence of siRNA2 (Fig. 5b,c). *In utero* coelectroporation of mut $GABA_{B2}$ together with siRNA2 rescued all phenotypes at P16 (Fig. 5d-g). Overexpression of mut $GABA_{B2}$ *per se* did not show any effect, in agreement with previous reports indicating that fully functional $GABA_{BR}$ s require coassembly of $GABA_{B1}$ and $GABA_{B2}$ subunits³.

Altogether, these data indicate that specific downregulation of endogenous $GABA_{B2}$ *in vivo* leads to increased axonal growth and decreased dendritic growth.

$GABA_{BR}$ mostly modulates cAMP signalling perinatally. Next, we investigated downstream effectors of $GABA_{BR}$ signalling responsible for the alterations in siRNA2-transfected animals. In adult animals, $GABA_{BR}$ s can decrease GABA and glutamate presynaptic release³. As standard *in utero* electroporation results in transfection of exclusively excitatory-neuron progenitors³¹, we excluded an increase in GABA release. On the other hand, we investigated whether $GABA_{BR}$ may modulate glutamate release

perinatally (P3-7) in the somatosensory cortex of wild-type (WT) animals. We recorded glutamate-mediated spontaneous excitatory postsynaptic currents (sEPSC) before and after bath application of $GABA_{BR}$ antagonist CGP55845 (CGP, 2 μM , to mimic presynaptic $GABA_{BR}$ downregulation; Fig. 6a). We found no difference in sEPSC frequency before and after CGP treatment (Fig. 3b). Conversely, CGP treatment increased sEPSC frequency at P18-19, as expected (Fig. 6a,b).

In adult animals, $GABA_{BR}$ s are also coupled to Kir channels. Therefore, in acute slices from animals transfected *in utero*, we recorded $GABA_{BR}$ -induced Kir currents in control WT or siRNac-transfected cells, and siRNA2-expressing cells by bath application of $GABA_{BR}$ agonist baclofen (50 μM) in the presence of $GABA_A$ R (bicuculline, 2 μM), glutamate receptor (kynurenic acid, 1 mM) and voltage-gated Na^+ channel (tetrodotoxin (TTX), 0.1 μM) inhibitors at P5-9 (Fig. 6c). In control neurons, baclofen-induced K^+ currents were negligible in comparison with adult levels (Kruskal-Wallis one-way analysis of variance (ANOVA), Dunn's method, $P < 0.05$) and did not differ from currents elicited in siRNA2-transfected cells ($P < 0.05$; Fig. 6c,d), confirming previous studies⁶.

We then reasoned that cAMP may be a possible effector upon $GABA_{BR}$ activation at perinatal ages. Interestingly, despite large

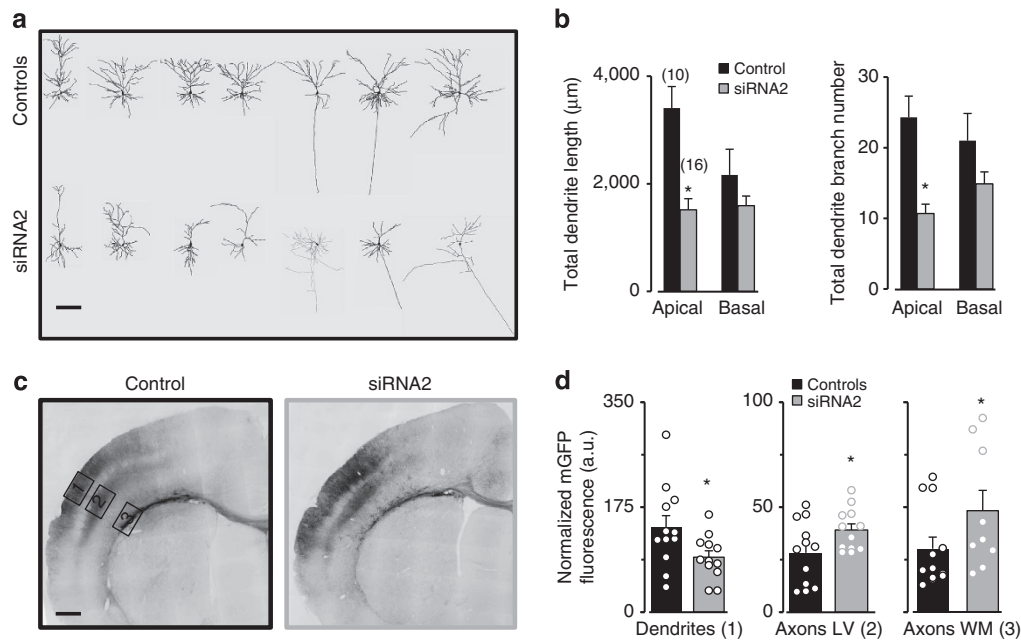


Figure 4 | GABA_{B2} downregulation significantly affects axon/dendrite growth in pyramidal neurons *in vivo*. (a) Neurolucida reconstruction of siRNA vector/Tomato (control) or siRNA2/Tomato pyramidal neurons filled with biocytin through a patch clamp pipette and located in layer II/III. Scale bar, 100 µm. (b) Quantification of the total dendritic length and branch number (separated for apical and basal dendrites) of all the cells reconstructed as in a. Asterisks indicate statistically significant difference compared with controls (one-way ANOVA, $P < 0.001$; *post-hoc* Holm-Sidak method, $P < 0.05$). Numbers in parentheses: number of cells analysed. (c) Confocal images of the fluorescence of plasma-membrane fusion protein mGFP in coronal sections of somatosensory cortices from P16 rats transfected *in utero* with mGFP, siRNA vector and Tomato constructs (control) or mGFP, siRNA2 and Tomato constructs. mGFP allows a better visualization of dendritic trees (boxed region 1) and thin and long axonal processes with branching and projection areas in deep cortical layer V (boxed region 2) and WM (boxed region 3). Scale bar, 500 µm. (d) Quantification of total mGFP fluorescence (normalized to the number of transfected Tomato-positive cells) in fields as in c. Data points represent results from single slices (hollow circles), and the average value (\pm s.e.m.) is indicated by the histogram (six animals each for control and siRNA2 experiments). Data for siRNA2 were significantly different (*) from those for controls (Mann-Whitney Test, $P < 0.05$).

literature on GABA_BR coupling to cAMP signalling in the adult neurons³, little evidence has been reported in young neurons³². To investigate this possibility in our system, we performed an ELISA immunoassay and measured cAMP levels after bath application of GABA_BR agonist baclofen (10 µM, pretreatment) or antagonist CGP (10 µM) in WT rat cortices acutely dissected at E17. We used adenylyl-cyclase activator forskolin (20 µM) as positive control. We found that both CGP and forskolin treatments significantly increased cAMP levels, whereas baclofen reduced forskolin-induced cAMP increase (Fig. 6e).

Altogether, these findings indicate that in the perinatal cortex GABA_BR is negatively coupled to cAMP signalling. Thus, the defects in migration and morphological maturation of pyramidal neurons were possibly due to impairment of cAMP signalling by GABA_BRs.

GABA_{B2}R siRNA affects *in vivo* neuronal development by cAMP/LKB1. cAMP is a key factor for axonal polarization and subsequent neuronal migration during perinatal development^{33–36}. In particular, cAMP and cGMP activities transduce the action of naturally polarizing extracellular factors on axon/dendrite formation through their reciprocal regulations³⁵. cAMP elevation causes cGMP decrease, promoting axon growth and specification, and suppressing dendrite formation, whereas cGMP elevation induces cAMP decrease and results in the opposite effects on axon/dendrite growth and polarization *in vitro*³⁵. Furthermore, *in vivo* manipulations that increased cAMP levels, as well as manipulations that decreased cGMP levels, were all accompanied by the same phenotypes that we described above for GABA_{B2}-siRNA-

electroporated animals^{34–36}. Thus, we hypothesized that elevation of cAMP levels together with reduction in cGMP levels may explain developmental defects by GABA_{B2} downregulation. Consequently, we investigated whether cGMP level was decreased in WT rat cortices (E17) by GABA_BR inhibition with CGP, due to reciprocal regulation with cAMP³⁵. As expected, cAMP elevation by GABA_BR inhibition was paralleled by decreased cGMP level in comparison with controls (Fig. 6f).

Then, we assessed GABA_BR involvement in cAMP/LKB1 signalling for regulation of axonal polarization *in vivo*. As the role of cAMP in axon initiation during neuronal polarization is regulated by phosphorylation of the downstream-kinase LKB1 at the protein kinase A (PKA)-site serine 431 (pLKB1-S431) (refs 34,37), we first assessed pLKB1-S431 in E21 cortices from WT non-transfected animals. Similar to GABA_{B2}R expression (Supplementary Fig. S1c), pLKB1-S431 was highly enriched at SVZ and CP (Fig. 7a). Second, we investigated whether pLKB1-S431 was increased by treatment with GABA_BR antagonist CGP (10 µM) in E17 WT freshly dissected cortices. We found that CGP treatment drastically increased pLKB1-S431 (Fig. 7b). Conversely, pretreatment with GABA_BR agonist baclofen (10 µM) significantly reduced forskolin-induced increase (Fig. 7b). Last, we directly investigated whether siRNA2 expression in E21 neurons at the SVZ affected pLKB1-S431. We found that siRNA2 expression (green) significantly increased pLKB1-S431 immunostaining (red) in transfected neurons, in comparison with control siRNAc neurons (green) (Fig. 7c).

If GABA_B downregulation effects *in vivo* were the result of increased activation of cAMP/LKB1 pathway, then overexpression of GABA_BR should rescue the effect of LKB1 overexpression on

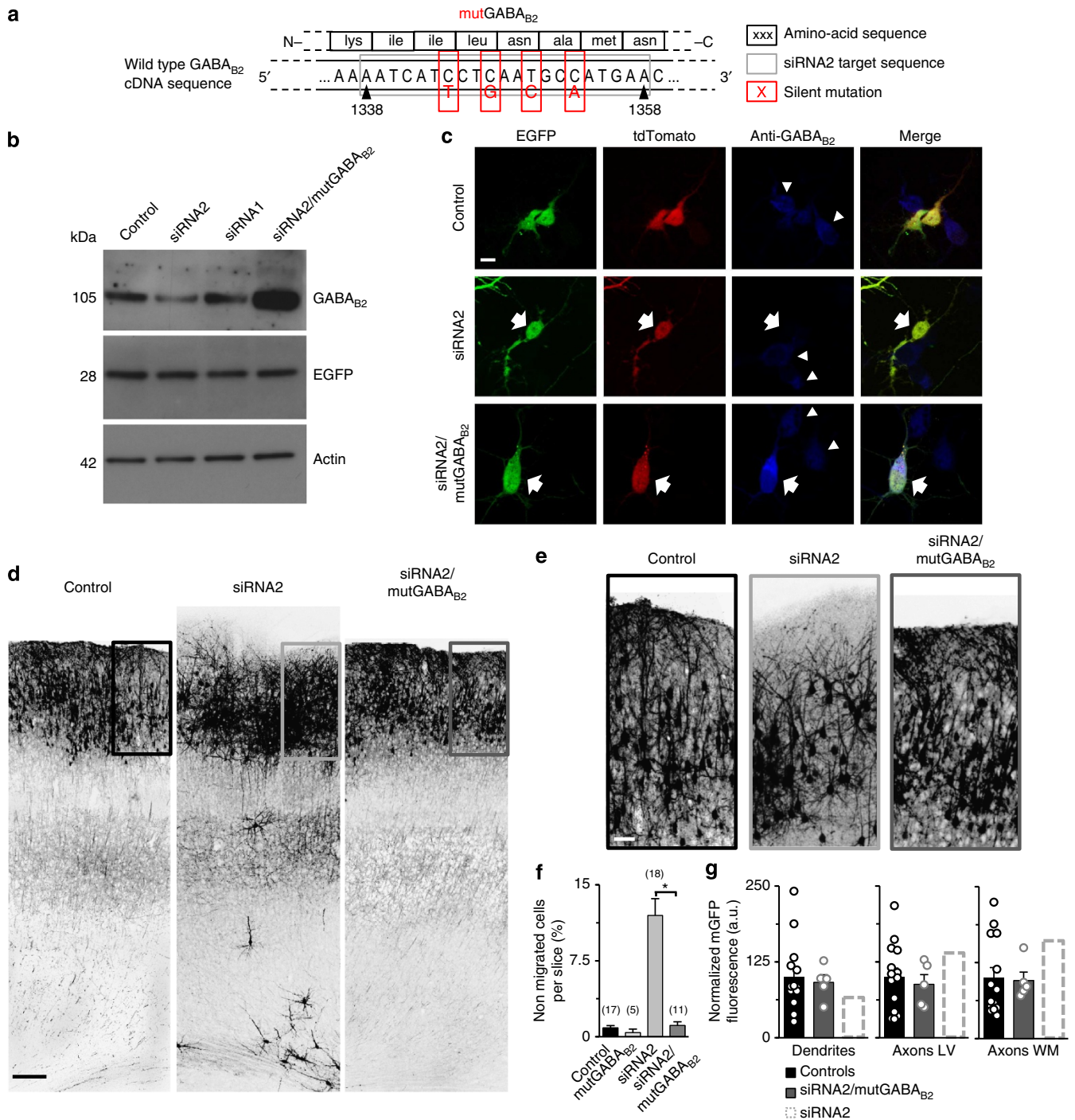


Figure 5 | siRNA-resistant GABA_{B2} rescues phenotypes associated with wild-type GABA_{B2}-subunit downregulation. (a) Cartoon exemplifying the four silent mutations (red) in the siRNA2-target sequence (grey) of the WT GABA_{B2} cDNA (black), which confer resistance to the siRNA2 and no change in the amino-acid sequence of the resulting protein (mutGABA_{B2}), compared with the WT. (b) Immunoblot with GABA_{B2} subunit specific antibody on total lysate of cortical neurons (3 DIV), transfected at plating with different vectors. Note the strong expression of GABA_{B2} subunit in cells expressing mutGABA_{B2}, despite co-transfection with siRNA2 (see Supplementary Fig. S10). (c) Immunostaining against GABA_{B2} (blue) in cortical cultures (3 DIV) confirmed the strong expression of GABA_{B2} in neurons transfected with mutGABA_{B2} (tdTomato fluorescence), even in the presence of siRNA2 (EGFP fluorescence). Arrows point to transfected neurons; arrowheads point to endogenous GABA_{B2} expression in non-transfected cells, for comparison. Scale bar, 25 μm. (d) Confocal images of tdTomato fluorescence in coronal sections of somatosensory cortices from P16 rats electroporated *in utero* at E17 with siRNA vector/Tomato (control), siRNA2/Tomato, and siRNA2 together with mutGABA_{B2}-Tomato (siRNA2/mutGABA_{B2}) constructs. Scale bar, 150 μm. (e) Higher magnifications of fields indicated in d. Scale bar, 40 μm. (f) Quantification of the number of neurons expressing either siRNA vector/Tomato or siRNAc/Tomato (controls, black), siRNA vector/mutGABA_{B2} (light grey), siRNA2/Tomato (dark grey) or siRNA2/mutGABA_{B2} (darkest grey) that did not complete their migration. The asterisk indicates statistically significant difference (Kruskal-Wallis one-way ANOVA, $P < 0.001$; *post-hoc* Dunn's method, $P < 0.05$). Numbers in parentheses: number of rats processed (1–2 averaged slices per rat). (g) Quantification of the total mGFP fluorescence intensity (normalized to the number of transfected Tomato-positive cells and control mGFP) of dendritic branching and axonal projecting areas as in Fig. 4c,d. The dotted rectangle represents data from siRNA-transfected cells from the experiment in Fig. 4d, and reported here as a reference for the magnitude of the rescue.

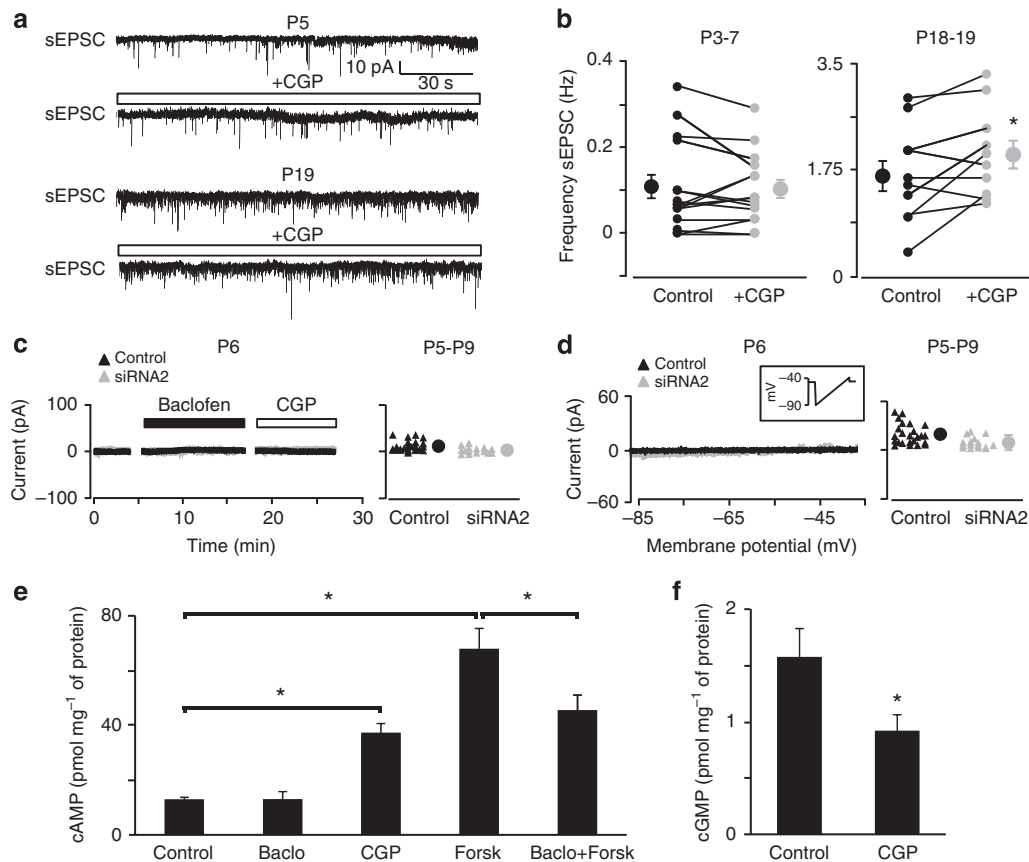


Figure 6 | GABA_BR predominantly modulates cAMP signalling during the first postnatal week. **(a)** Examples of glutamate-mediated sEPSC in whole-cell patch clamp recordings from neurons in layer II/III of the somatosensory cortex (recorded in bicuculline 25 μM, P5 or at -70 mV, P19) before and during bath application of GABA_BR antagonist CGP (2 μM). **(b)** Quantification of the frequencies of sEPSCs before (control) and after bath application of CGP (+CGP), recorded as in **a**. sEPSC frequency was increased by CGP application only at P18-19 (*, paired *t*-test, *P* = 0.04). Each symbol represents one recorded cell and the average ± s.e.m. is reported on the side. Lines connect data from the same cell. **(c)** Examples of whole-cell patch clamp recordings showing Kir currents obtained by bath application of GABA_BR agonist baclofen (50 μM) and antagonist CGP (2 μM) in acute cortical slices from a WT control (black) and a siRNA2 (grey) transfected cell at P6. The graph on the right represents the amplitude of currents measured in all recorded cells (triangles) after 10 min bath application of baclofen as in the example. The average ± s.e.m. is reported on the right (circle). **(d)** Examples of whole-cell patch clamp recordings during a ramp test protocol (from -90 to -40 mV, 500 ms, inset) in the same set of cells as in **c**. The graph on the right represents the peak amplitude of baclofen-induced currents measured in all recorded cells (triangles) as in the example. The average ± s.e.m. is reported on the right (circle). Peak amplitudes were calculated as in Fig. 1d. **(e)** ELISA measurement of the cAMP level following bath application of vehicle (control), baclofen (10 μM), CGP (10 μM), forskolin (20 μM) or baclofen + forskolin to cortices acutely dissected at E17, in 5-14 independent experiments. Asterisks: statistically significant difference (One-way ANOVA, *P* < 0.001; *post-hoc* Holm-Sidak method, *P* < 0.05). **(f)** ELISA measurement of the cGMP level following bath application of CGP (10 μM) in nine independent experiments as in **e**. CGP-treated cortices significantly differed (*) from controls (Mann-Whitney Test, *P* = 0.013).

migration and axonal development^{34,35}. Therefore, we performed *in utero* electroporation of control EGFP/Tomato, LKB1-EGFP/Tomato (Supplementary Fig. S2e) or LKB1-EGFP together with GABA_{B1}-Tomato (both isoforms B1a and B1b, Supplementary Fig. S2g) and mutGABA_{B2}-Tomato (to ensure expression of a functional GABA_BR), and examined the number of ectopic cells and axonal development at P16. *In utero* coelectroporation of two expression vectors with the same promoter resulted in coexpression of the two proteins encoded by the vectors with a tight correlation (Supplementary Fig. S4b,d; Pearson product moment correlation, *R* = 0.98 ± 0.01; *n* = 6 animals). Overexpression of LKB1 and GABA_B subunits in neurons resulted in functional proteins (Supplementary Figs S6 and S7). In line with GABA_{B2}R downregulation, LKB1 overexpression *in vivo* resulted in ectopic cells and increased fluorescence in axonal-projection regions at P16 (Fig. 7d,e and f), as previously described³⁴. Interestingly, overexpression of GABA_BR

(GABA_{B(1&2)}) together with LKB1 significantly rescued all these LKB1-induced effects. Moreover, upon expression of a constitutively active LKB1 phosphomimetic mutant at the PKA site (also affecting neuronal migration and axonal development; LKB1S431E), we found that GABA_BR overexpression was not able to rescue LKB1S431E overexpression-induced defects (Fig. 7d,e and f). Thus, GABA_BR exerted its role on LKB1 through the cAMP/PKA pathway. Conversely, GABA_{B(1&2)} overexpression *per se* had no effect on migration or morphological maturation (Fig. 7d,e and f). That GABA_{B2}-siRNA affected neuronal migration and morphological maturation by LKB1 signalling was confirmed by the fact that *in utero* coelectroporation of LKB1-siRNA³⁴ and siRNA2 rescued the developmental phenotypes (Supplementary Fig. S8).

Altogether, these findings indicate that GABA_BRs affect migration and axonal development by modulation of cAMP/LKB1 pathway *in vivo*.

GABA_{B2}R siRNA affects axon/dendrite polarization *in vitro*.

Next, we investigated whether activation of GABA_BR and consequent cAMP/LKB1 signalling specifically affected axon/dendrite polarization. Unfortunately, immunostaining of abnormal processes with axon-specific markers in SVZ and ectopic multipolar siRNA2 neurons was not successful due to dense staining from non-transfected cells. Thus, we turned to cell cultures as a simplified system, as in other *in vivo* studies^{34–38}. Indeed, similarly to polarization *in vivo*, neuronal maturation in culture undergoes polarization from a morphologically symmetric cell with multiple equivalent neurites to a polarized neuron exhibiting a single axon and multiple dendrites³⁰. Therefore, we prepared primary cortical neuronal cultures and examined the effect of GABA_BR modulation by treatment with GABA_BR agonist baclofen (10 μM) and antagonist CGP (10 μM) 3 h after plating, or by transfection with siRNA2 at plating (Fig. 8a). At this stage, neurons in culture are not polarized (no axonal immunoreactivity for Smi-312, red), but exhibit multiple equivalent processes all immunopositive for GABA_{B2} (green, Supplementary Fig. S1e). As positive control, we treated cultures with forskolin (20 μM). As axon/dendrite polarization is tightly linked to neurite growth³⁵, we first assessed the relative length and branch numbers of axons and dendrites in treated neurons at 3 DIV, when cells have acquired a polarized morphology. Cells treated with baclofen and transfected with siRNA (EGFP) vector for visualization had longer and more branched dendrites (MAP2 staining) associated with shorter and less branched axons (Smi-312 staining; Fig. 8b,c). Conversely, siRNA2 transfection or treatment with either CGP or forskolin resulted in shorter dendrites and longer axons, compared with control cells treated with vehicle (dimethylsulphoxide 0.1%) and transfected with either siRNA empty vector or siRNAc (Fig. 8b,c).

Furthermore, to address whether GABA_BR signalling modulates axonal specification, we quantified the number of cells with one axon (SA), no axon (NA) or multiple axons (MAs) in cortical cultures (Fig. 8d). The percentages of SA, NA and MA cells in control conditions were $76.2 \pm 1.4\%$, $18.6 \pm 1.3\%$, $5.1 \pm 0.2\%$, respectively (Fig. 8e). Interestingly, bath application of baclofen strongly increased the percentage of NA cells and decreased the percentage of MA cells (Fig. 8e). Conversely, bath application of either CGP or forskolin, or siRNA2 transfection, increased the percentage of MA cells (Fig. 8e). Figure 8f represents samples of reconstructed neurons from drug-treated cultures.

To address whether GABA_BR signalling specifically affected axonal initiation, we prepared cortical cultures plated on stripe substrates of a membrane-permeable fluorescent analogue of cAMP (F-cAMP, 20 μM), GABA_BR agonist baclofen (1 μM, together with fluorescent bovine serum albumin (F-BSA; 5 μM)), GABA_BR antagonist CGP (1 μM, with F-BSA) or control F-BSA, which is a well-established method for studying axonal specification^{34–36,38}. Immunostaining of neurons at 4 DIV with axon-marker Smi-312 and neuronal marker Tuj-1 (Fig. 8g), revealed that for all polarized neurons with the cell body located at a stripe boundary, the presence of GABA_BR agonist baclofen resulted in a large increase of axon initiation off the baclofen stripe, as exemplified by the high preference index (PI, defined as $(\% \text{ on stripe}) - (\% \text{ off stripe}) / 100$; Fig. 8h). Notably, some axons revealed growth repulsion from baclofen stripes, as previously reported for cGMP stripes^{34,35} (Fig. 8g). Conversely, polarized neurons with the cell body located at the boundary of either CGP or F-cAMP stripes exhibited large axon initiation on the stripes. Interestingly, a causal link between GABA_BR and cAMP decrease was demonstrated by the fact that the PI returned to control levels when cell cultures on baclofen stripes were treated with forskolin (20 μM; Baclo + Forsk) or when cell cultures on CGP stripes were treated with adenylyl-cyclase inhibitor SQ22536 (10 μM; CGP + SQ; Fig. 8h).

Altogether, these data are in agreement with the *in vivo* experiments and identify GABA_BR as a modulator of axon/dendrite growth and polarization by inhibition of cAMP signalling.

Discussion

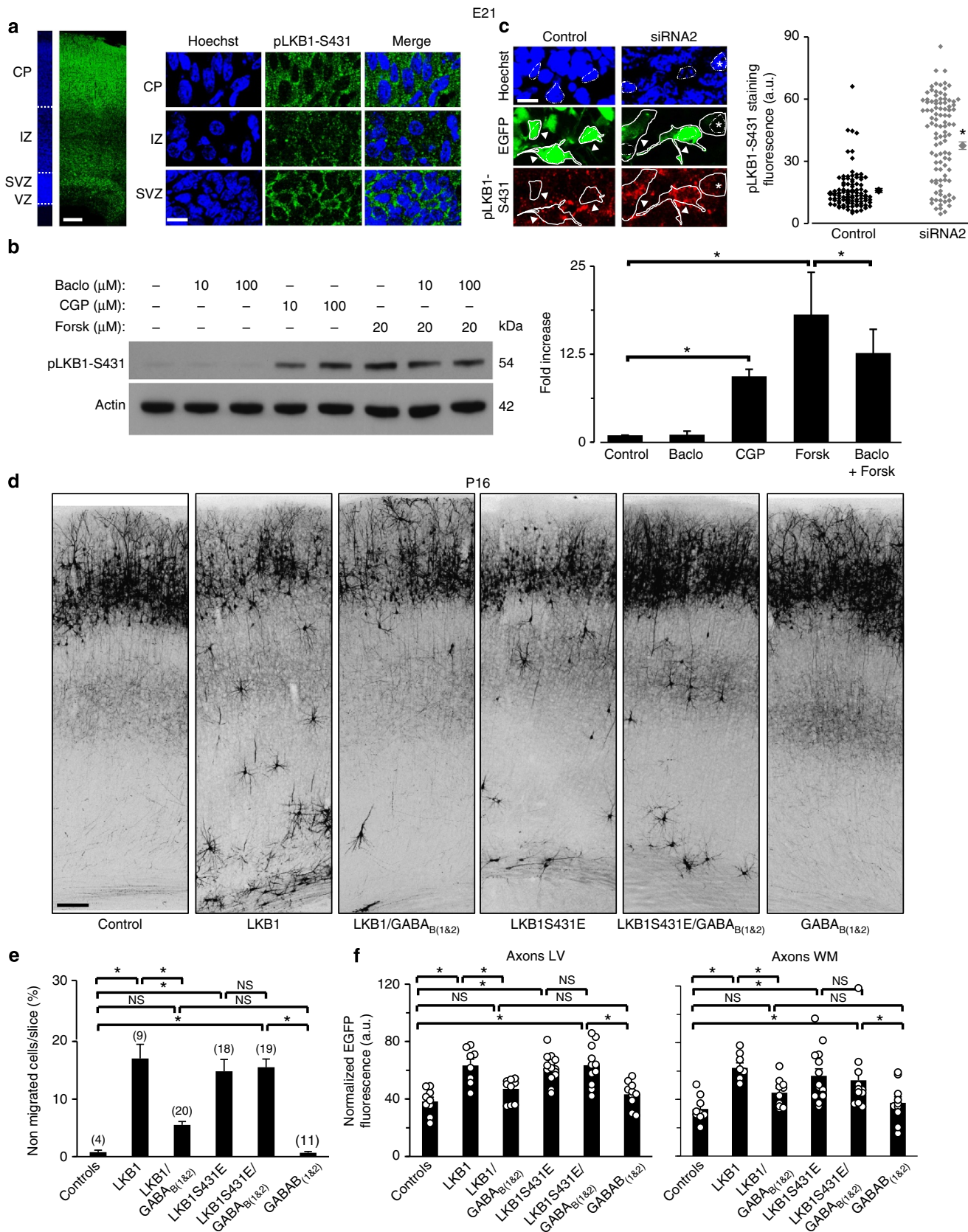
Here, we coupled siRNA to *in utero* electroporation to downregulate endogenous GABA_{B2} in a subpopulation of newly born cortical neurons and determine *in vivo* function of this receptor for neurons in their native environment. We found that GABA_{B2} downregulation *in vivo* impaired radial migration and morphological maturation of cortical neurons by modulation of cAMP/LKB1 pathway. Our *in vitro* studies demonstrated that the specific morphological effects on axon and dendrites derived from a defect in neuronal polarization.

Developing neural tissues are enriched in GABA^{1,2}. In particular, as interneurons migrate tangentially in cortical IZ, GABA-positive cells increase in number and establish gradients of secreted GABA that migrating excitatory neurons sense through GABA_A (ref. 6), but possibly also GABA_B receptors (Supplementary Fig. S9). GABA concentration in the developing brain remains even higher due to immature blood–brain barrier³⁹ and re-uptake system⁴⁰, leading to tonic activation of GABA_ARs²⁹. Interestingly, tonic GABA_Aergic signalling is not hyperpolarizing but depolarizing and mostly excitatory during development^{1,2,4}, and glutamatergic-system development lags behind. This allows to excite developing neurons for maturation, while avoiding the toxic effects of a mismatch between GABAergic inhibition and glutamatergic excitation⁷. Here, we showed that also GABA_BR signalling is not hyperpolarizing in early development, in keeping with above. Moreover, we indirectly provided evidence that also GABA_BRs are under tonic activation by endogenous GABA at this age. Indeed, despite the abundance of GABA_BR that we and others found in the cortex^{8,32}, application of GABA_BR agonist baclofen to embryonic cortices did not decrease basal level of cAMP and pLKB1-S431. Conversely, blockade of endogenous GABA_BR by antagonist CGP revealed a significant effect. We hypothesize that the lack of baclofen effect on basal cAMP and pLKB1-S431 was due to high concentration of endogenous GABA in the developing tissue that may tonically saturate GABA_BR responses, conversely, unmasked by CGP application. Accordingly, in cell cultures (10% of GABAergic interneurons; Supplementary Fig. S1d) where endogenous GABA concentration is likely diluted by the cell medium, baclofen generated larger effects than CGP treatment or siRNA2 transfection. This is demonstrated by the fact that: (1) baclofen treatment affected both axonal length and branch number, whereas CGP treatment or siRNA2 transfection affected axonal length only. (2) Baclofen treatment affected MA and NA cell populations, whereas CGP treatment or siRNA2 transfection affected MA population only. (3) Baclofen stripes occasionally induced a repulsion effect for axonal growth, whereas the predicted attraction effect was never found for CGP stripes. (4) PI of axon initiation for repulsive baclofen stripes was ~1.5 fold larger than that for attractive CGP stripes.

Despite some contrasting results by few previous studies, there is general agreement that GABA_BR signalling affects axonal growth and modulates neuronal migration *in vitro*^{9,10}. In particular, in line with our data, GABA_BR antagonist delayed migration of excitatory neurons from the IZ to the CP¹⁷, and produced accumulation of tangentially migrating interneurons (associated with a shorter leading neuronal process) in the VZ/SVZ of organotypic cortical slices independently of Kir channels¹⁵. Conversely, *in vivo* studies in a number of genetically modified mice with targeted deletion or upregulation of GABA_{B1}

or GABA_{B2} indicated no gross brain-morphology abnormalities⁶. The defects in GABA_BR-downregulated neurons seen here and in the *in vitro* literature may depend on the different experimental manipulations and knockdown timing. Indeed, delivery of siRNA

in utero at E17 or in cell cultures at 0 DIV *versus* life-long deletion or long-term overexpression of GABA_BR in genetically modified mice may favour compensatory mechanisms in the latter case. Additionally, one must distinguish between manipulations of the



global network (GABAergic system included) in genetically modified mice, *versus* manipulations in individual excitatory neurons within a normally developing network, as in our study. Finally, developmental defects in GABA_BR genetically modified mice may have been simply overlooked due to *in vivo* system complexity. Indeed, the epileptic phenotype observed in adult mice knockout for the GABA_{B1} subunit (lacking the inhibitory hyperpolarization by GABA_B activation of Kir3.2) is more severe than that observed in the weaver mouse (mutated Kir3.2 channels) or in the Kir3.2 knockouts^{19,41–43}. This suggested that GABA_BR modulation of downstream effectors other than Kir3.2 channels may provide a critical component of GABA_BR signalling during development^{20,41,44}, as confirmed here for cAMP/LKB1 pathway.

We found that GABA_BR mainly regulates cAMP levels during early development. We concluded that GABA_BR is a modulator of neuronal polarization *in vivo* through cAMP/LKB1 pathway based on the following evidence: (1) *in vitro* GABA_{B2} down-regulation affected axon/dendrite growth and polarization by cAMP pathway; (2) *in vivo* defects due to GABA_{B2}-siRNA phenocopied the effects upon increase of cAMP/LKB1 signalling *in vivo*^{34–36}, (3) *in vivo* GABA_BR overexpression significantly rescued LKB1- (but not phosphomimetic LKB1-S431E) overexpression effects. Accordingly, GABA (through GABA_BR signalling) shares similarities with polarization molecules. First, GABA_BR is abundantly expressed at the level of the VZ/SVZ, where neuronal polarization takes place. Second, like other polarizing molecules (for example, TGFβ)³⁸, GABA is possibly expressed in a steep gradient (above the SVZ) by GABAergic cells tangentially migrating in the cortex (Supplementary Fig. S9). However, in strong contrast with active determinants³³ of neuronal polarization (for example, LKB1), which *in vitro* show axonal-fate predictive-accumulation in one single process at a time when neurons are yet not polarized³⁴, GABA_BR showed similar expression in all non-polarized neurites in cultured neurons. We hypothesize that at SVZ, in unpolarized neurons expressing GABA_BR equally in all neurites, the process facing the CP (future dendrite) be more likely to sense higher concentration of GABA translated in low cAMP level by GABA_BRs. Thereby, GABA_BR would inhibit axonal formation by low cAMP, while favoring dendrite formation by high cGMP level (Supplementary Fig. S9, inset)³⁵. Thus, beside determinants of neuronal polarization (for example, LKB1) and natural polarizing factors³³ (for example, neurotrophins, semaphorins), we postulate *in vivo* the existence of molecules such as GABA that simply modulate³³ the polarization process due to specific temporal (for example, GABA released from migrating

interneurons at E18) and spatial (migrating interneurons located above polarizing excitatory cells) cues (Supplementary Fig. S9). The hypothesis that GABA_BR signalling may act as a modulator³³, rather than a determinant of neuronal polarization *in vivo* is further strengthened by the fact that, while overexpression of LKB1 lead to defective polarization *in vivo*, overexpression of GABA_B subunits did not. This indicates that the gradient generated by the migrating interneurons may possibly be the ultimate responsible for the polarization effect in GABA_{B2}-siRNA animals. Thus, proper development of neural network *in vivo* may indeed require accumulation of active determinants of neuronal polarization³³ (for example, LKB1) at the bipolar stage, but with respect to coordinates by external cues in the surrounding tissue (for example, GABA from migrating interneurons) modulating final polarization commitment⁴⁵. Therefore, we cannot exclude that at other stages or in other brain regions characterized by different cellular environments GABA_BR activation may be functional to different developmental processes.

Is the defect in neuronal polarization also important for migration of newborn neurons? As neuronal polarization *in vivo* occurs before radial migration, migration defects may be attributed in part to the axonal polarization defect in GABA_B-siRNA cells, as already hypothesized in other studies^{34–36,46}. In support of this idea, we note that only cells displaying bipolar morphology were located at the CP for GABA_{B2}-siRNA neurons, and that these cells also expressed lower levels of GABA_{B2}-siRNA. Moreover, ectopic neurons were the most morphologically affected. However, we cannot exclude that failure in radial migration may be due to the reduced length in apical dendrites. Finally, we indicate cAMP/LKB1 signalling as responsible for the described effects on newborn cortical neurons. However, we cannot exclude the participation of some of the other signalling pathways downstream of GABA_BR^{34,47–51}.

In conclusion, our study revealed an unknown function for GABA_BR through cAMP/LKB1 pathway during early cortical development. This drives attention on possible side effects of the clinical use of centrally acting drugs such GABA_BR agonist baclofen (a myorelaxant and painkiller) or substances that increase extracellular levels of GABA (many antiepileptics) in pregnant women and children.

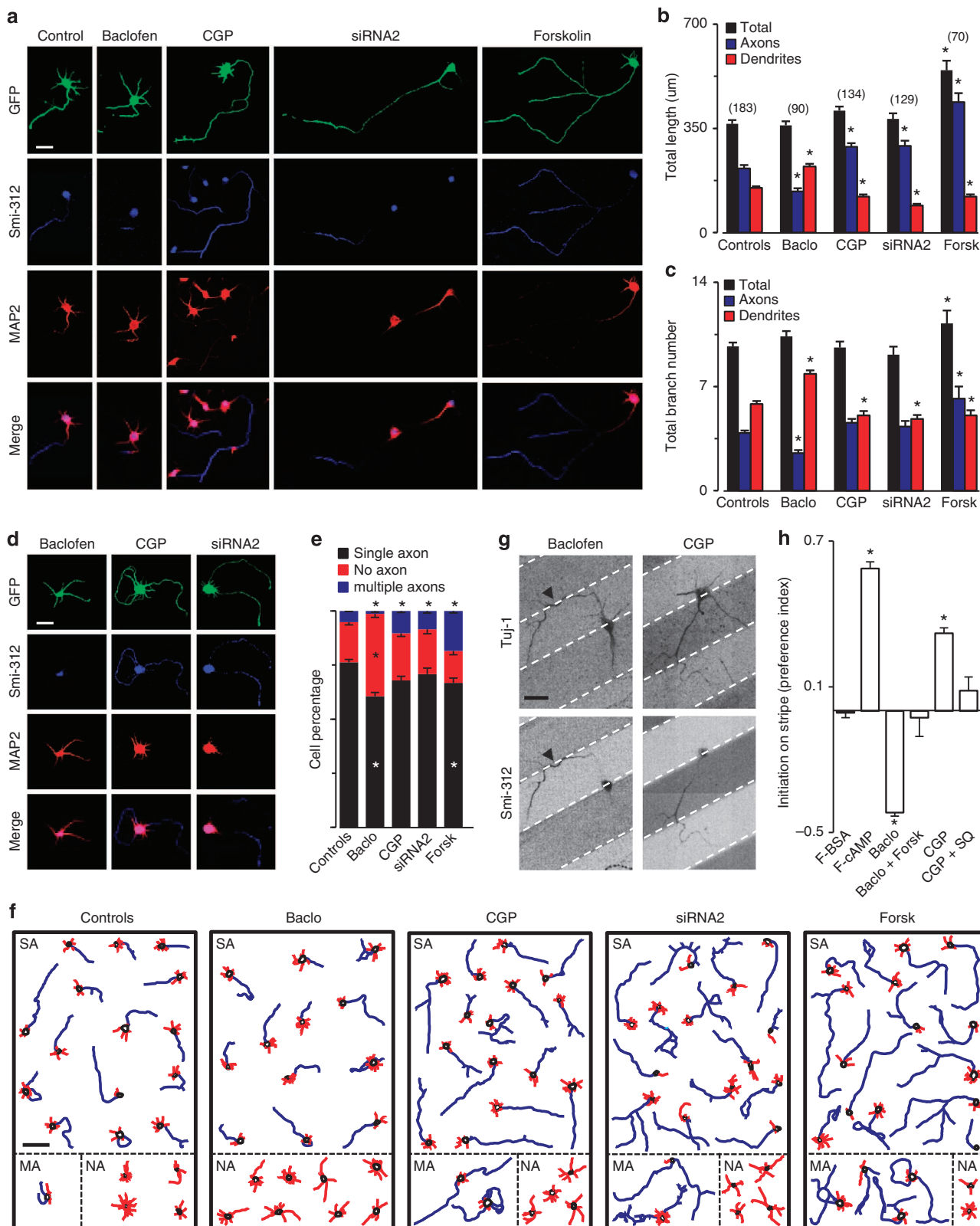
Methods

Generation of siRNAs and plasmid constructs. We generated two 21-oligonucleotide siRNA duplexes targeting rat GABA_{B2} subunit (starting position: 1,338, seq no. 1; 975, seq no. 2). For mutGABA_{B2} vector, we created a siRNA-resistant GABA_{B2} cDNA by introducing four silent mutations in the siRNA2-target sequence of rat GABA_{B2} cDNA (gift of Dr Kaupmann, Novartis Pharma AG, Basel;

Figure 7 | GABA_BR regulates neuronal development *in vivo* through cAMP/LKB1 signalling. (a) Left: confocal image of LKB1 phosphorylation at PKA-site serine S431 (pLKB1-S431) immunostaining (green) from a coronal section of rat somatosensory cortex at E21. Slices were counterstained with Hoechst (blue). Scale bar, 100 μm. Right: high-magnification images of SVZ, IZ and CP. Note the abundance of pLKB1-S431 in SVZ and CP. Scale bar, 10 μm. (b) Left: western blot showing pLKB1-S431, upon bath application of vehicle (control), baclofen, CGP and forskolin to cortices acutely dissected at E17 (see Supplementary Fig. S10). Right: quantification of the fold-increase average of pLKB1-S431 compared with control, in five independent experiments as in left. GABA_BR inhibition by CGP (10 μM) increased pLKB1-S431, mimicking forskolin treatment (Kruskal-Wallis one-way ANOVA on ranks, $P < 0.001$; *post-hoc* Student–Newman–Keuls method, $P < 0.05$). Conversely, pretreatment with baclofen (10 μM) significantly reduced forskolin-induced pLKB1-S431 ($P < 0.05$). (c) Confocal images of pLKB1-S431 immunostaining (red) and nucleus staining (Hoechst, blue) from a coronal SVZ section of a rat at E21 previously transfected with control siRNAs (green) or siRNA2 (green). Arrowheads point to highly transfected cells, whereas the asterisk marks a low transfected cell for comparison. Scale bar, 10 μm. Right: average cytoplasmic fluorescence measured at the cell body for all cells analysed (diamonds; three animals each per experimental case) as in the example on the left. The average ± s.e.m. is reported on the right. The asterisk indicates statistically significant difference (Mann–Whitney test $P < 0.001$). (d) Confocal images of EGFP fluorescence in coronal sections of somatosensory cortices from P16 rats transfected *in utero* with the indicated constructs. Scale bar, 150 μm. (e) Quantification of the percentage of neurons that did not complete their migration at P16 in slices from animals transfected with the indicated constructs. Asterisks indicate statistically significant difference (Kruskal–Wallis one-way ANOVA, $P < 0.001$; *post-hoc* Dunn’s method, $P < 0.05$). Numbers in parentheses: number of rats processed (1–2 averaged slices per animal). (f) Quantification of the average EGFP fluorescence intensity (normalized to the number of transfected Tomato-positive cells and field background) of axonal projecting areas, as in Fig. 4c. NS, not significant.

NM_031802) with the QuickChange lightning mutagenesis kit (Stratagene, La Jolla, CA). PCR-based strategies were used to generate the serine-to-glutamic acid point mutation of LKB1 at the PKA-site Ser431 (LKB1S431E). Lymphocyte-specific-kinase membrane-anchor domain (aLCK)-GFP vector (gift of Dr Canossa), allowed expression of aLCK-GFP fusion protein that localizes at the plasma membrane (mGFP), and was used for better visualization of thin neuronal processes *in vivo*.

In utero electroporation. Timed-pregnant Sprague Dawley rats (Harlan Italy SRL, Correzzana, Italy) were anaesthetized at E17 with isoflurane (induction, 3.5%; surgery, 2.5%), and uterine horns were exposed by laparotomy. Expression vectors ($1-2 \mu\text{g} \mu\text{l}^{-1}$ /Vector in water) and dye Fast Green (0.3 mg ml^{-1} ; Sigma, St. Louis, MO) were injected ($5-6 \mu\text{l}$) through the uterine wall into one of the embryos' lateral ventricles by a 30-G needle (Pic indolor, Grandate, Italy). Each embryo's head was held between tweezer-type electrodes (10 mM diameter; Nepa Gene,



Chiba, Japan) across the uterus and five electrical pulses (amplitude, 50 V; duration, 50 ms; intervals, 100 ms) were delivered with a square-wave electroporation generator (CUY21EDIT; Nepa Gene). Uterine horns were returned into the abdominal cavity, and embryos continued their normal development. For later identification, control embryos were injected in the left ventricle, whereas experimental embryos in the right ventricle. Experiments were approved by IIT licensing and Italian Ministry of Health.

Slice histology. E18–P1 brains were directly fixed in 4% paraformaldehyde (PFA in PBS). P2–P16 brains were fixed by transcardial perfusion of 4% PFA. Brains were sectioned coronally 80- μ m thick with a vibratome (Leica VT1000S). Free-floating slices were permeabilized and blocked with PBS containing 0.3% Triton X-100, 10% NGS and 0.2% BSA. Primary antibodies were incubated in PBS containing 5% NGS and 0.1% BSA (guinea pig anti-GABA_{B2} 1:1,500 (Millipore, Billerica, MA); rabbit anti-GABA 1:1,000 (Sigma); rabbit anti-pLKB1-S431 1:100 (Santa Cruz) with peptide-LKB1 preincubation (1:50, 30 min)). Immunostaining was detected using Alexa fluorescent secondary antibody 1:600 (Invitrogen) in PBS containing 5% NGS. Slices were counterstained with Neurotrace Nissl 640/660 (1:100; Invitrogen Corporation, Carlsbad, CA) or Hoechst (2.5 μ g μ l⁻¹; Sigma). Samples were mounted in Vectashield (Vector Laboratories, Inc., Burlingame, CA) and examined with confocal microscopy.

For biocytin experiments, we used 400- μ m-thick acute slices from patch clamp recordings where biocytin (3–4 mg ml⁻¹, Sigma) was added in the pipette solution. Slices were fixed in 4% PFA. Revelation of biocytin-injected neurons was obtained with Vectastain ABC Elite kit (Vector Laboratories), and slices were mounted in Mowiol (Calbiochem, La Jolla, CA). Biocytin-filled neurons were drawn by using a camera lucida (Olympus, Düsseldorf, Germany) and were computer reconstructed and analysed using NeuroLucida and NeuroLucida explorer (MicroBrightField, Colchester, VT).

Confocal and NeuroLucida image acquisition and analysis. For analysis of migration at E21–P16, images from sections counterstained with Neurotrace Nissl 640/660 or Hoechst staining were acquired on a confocal laser-scanning microscope (TCS SP5; Leica Microsystems, Milan, Italy) equipped with a \times 10 immersion objective (numerical aperture (NA) 0.3). Confocal images (15- μ m-thick z-stacks) were acquired, and Z-series were projected to two-dimensional representations. The contrast of the images was adjusted to enhance the fluorescence of cell bodies, while attenuating the signal from neuronal processes to facilitate cell counting. For quantification of non-migrating cells, all cells in the VZ/SVZ, IZ or CP were counted and normalized to the total number of cells in the slice. Two-three slices were acquired for each animal and averaged together. For high-magnification images of cell morphology, 80- μ m-thick z-stacks were acquired with a \times 63 immersion objective (NA 1.4), and Z-series were projected to two-dimensional representations. In some experiments, we took advantage of mGFP fusion protein (for quantification of neurite processes) and transfected it together with Tomato (for counting of the number of transfected cells). For mGFP (Figs 4 and 5, Supplementary Fig. S8) or EGFP (Fig. 7) quantification of axons and dendrites, six confocal images/slice (one single focal plane for both mGFP and tdTomato fluorescence at the level of brightest tdTomato fluorescence) were acquired (\times 10 objective, NA 0.4, or \times 20 objective, NA 0.5) for fields at the layer II/III, layer V and white matter (as indicated in Fig. 4) of transfected animals. Total mGFP or average EGFP fluorescence was calculated for each field with the Leica LAS AF Lite software (Leica Microsystems for fluorescence), and normalized to the total number of transfected (tdTomato) positive (mGFP, EGFP) cells and to slice background (EGFP). For cell-culture experiments, confocal images (one single focal plane at level of the brightest EGFP fluorescence) were acquired with a \times 40 immersion objective (NA 1.25). For each litter of animals or cell-culture experiment, all slides were acquired in a random order and in a single session to minimize errors caused by fluctuation in laser output and degradation of

fluorescence. For correlation analysis of different fluorescence level in slices (Fig. 2; Supplementary Fig. S4), cells were acquired with a \times 40 immersion objective (one single focal plane at the level of brightest tdTomato fluorescence, for cells at CP and ectopic neurons). All experiments were acquired and analysed in a blind manner.

Electrophysiology. Coronal somatosensory cortical slices were acutely isolated from rats (400 μ m thick) in ice-cooled cutting solution with the following composition (in mM): 0.1 MgCl₂; 2.5 KCl; 1.25 NaH₂PO₄; 2 MgSO₄; 0.1 CaCl₂; 26 NaHCO₃; 206 sucrose and 12 D-glucose (\sim 300 mOsm, pH 7.4), oxygenated with 95% O₂ and 5% CO₂. Slices were incubated in artificial cerebrospinal fluid (ACSF) with the following composition (in mM): 124 NaCl; 2.5 KCl; 1.25 NaH₂PO₄; 2 MgSO₄; 2 CaCl₂; 26 NaHCO₃ and 12 D-Glucose (\sim 310 mOsm, pH 7.4), oxygenated with 95% O₂ and 5% CO₂. After 1-h recovery, slices were used under continuous perfusion of ACSF at room temperature. Whole-cell patch clamp recordings were made with a Multiclamp 700B amplifier (Molecular Devices). Data were sampled at 20 KHz, filtered at 5 KHz, and analysed off-line with Clampfit software (Molecular Devices).

Cell culture and transfection. In neuronal cell-culture experiments, cell density was 25,000 cells per cm² for immunostaining experiments, and 7,500 cells cm⁻² for stripe experiments (Supplementary Information). Primary cultures of dissociated cortical neurons were prepared from E18 rat embryos and maintained in Neurobasal medium supplemented with: 2% B-27 supplement, 0.5 mM glutamine, 50 μ g ml⁻¹ of penicillin and 50 μ g ml⁻¹ of streptomycin (Invitrogen). For measurements of neurite or axon/dendrite lengths, and SA MA and NA classification, cells were treated with forskolin (20 μ M), baclofen (10 μ M), CGP55845 (10 μ M), SQ22536 (10 μ M) starting 3 h after plating, and drugs were present throughout the duration of the experiment. Cells (4×10^6) were transfected before plating by electroporation with Amaxa basal nucleofactor kit for primary neurons (Lonza; transfection efficiency = 80–90% of total neurons) by 3–4 μ g of plasmid DNA in the Amaxa nucleofactor device (program 003) according to the manufacturer's protocol.

Immunostaining. For immunostaining, neurons were fixed with 4% PFA in PBS for 15 min, followed by 15-min treatment with 0.1% Triton X-100, and 2 h blocking with 10% NGS. Primary antibodies (guinea pig anti-GABA_{B2} 1:1,500 (Millipore); rabbit anti-GABA 1:1,000 (Sigma); rabbit anti-MAP2 1:3,000 (Covance, Research Products, Inc., Berkeley, CA); mouse anti-Smi-312 1:800 (Covance); chicken anti- β III tubulin 1:1,000 (Millipore); rabbit anti-pLKB1-S431 1:100 (Santa Cruz) with preincubation of LKB1 peptide (1:50, 30 min); mouse anti-Nestin 1:100 (Abcam); rabbit anti-CDP (Cux1) 1:100 (Santa Cruz) were incubated in PBS containing 5% NGS. Fluorescently conjugated secondary antibodies (Alexa 488, Alexa 568 and Alexa 647 at 1:1,000, or CY5 at 1:100 (Jackson ImmunoResearch Laboratories, West Grove, PA, USA)) were incubated in PBS containing 5% NGS. Samples were counterstained with Hoechst (2.5 μ g μ l⁻¹), mounted in Vectashield (Vector Laboratories, Inc., Burlingame, CA), and examined with confocal microscopy (see above), followed by neurite tracing and quantification with the NeuronJ plugin of ImageJ software (NIH, <http://rsb.info.nih.gov/ij/>)⁵².

cAMP and cGMP measurements. Levels of cAMP and cGMP in rat freshly dissected cortices (E17) were measured with cAMP and cGMP EIA kits (Cayman Chemical). After 2 h recovery in ACSF oxygenated with 95% O₂ and 5% CO₂, baclofen and CGP were preincubated (15 min, room temperature) before bath application of forskolin (15 min).

Figure 8 | GABA_{B2} downregulation affects axon/dendrite growth and polarization of cortical neurons *in vitro*. (a) Cultured cortical neurons (3 DIV) immunostained for axons (Smi-312, blue) and dendrites (MAP2; red). Cells were treated with vehicle (control), baclofen (10 μ M), CGP (10 μ M) or forskolin (20 μ M) 3 h after plating, or transfected with siRNA2 at plating. All drug-treated neurons were transfected with siRNA (EGFP) vector or siRNAC for visualization. Scale bar, 50 μ m. (b) Total neurite length and axonal and dendritic relative lengths of neurons as in a. Asterisks: significant difference compared with controls (one-way ANOVA, $P < 0.001$; *post-hoc* Dunn's method, $P < 0.05$). (c) Total branch number and axonal and dendritic relative branch numbers of the data set in b. Asterisks: significant difference compared with controls (Kruskal-Wallis One-way ANOVA, $P < 0.001$; *post-hoc* Dun's method, $P < 0.05$). (d) Neurons presenting no axon (baclofen) or multiple axons (CGP, siRNA2), following treatment as in a. Scale bar, 50 μ m. (e) Percentage of neurons (four independent experiments, \sim 250 cells per condition) as in a and d, characterized by one single axon (black), no axon (red) and multiple axons (blue). Asterisks: significant difference compared with controls (one-way ANOVA, $P < 0.001$; *post-hoc* Holm-Sidak method, $P < 0.05$). (f) Neurons reconstructed for each condition as in a with location of the cells artificially arranged for axon (blue) and dendrite (red) display. SA, single axon; MA, multiple axons; NA, no axon. Scale bar, 100 μ m. (g) Neurons cultured on a substrate coated with stripes (dark grey) of baclofen (1 μ M) or CGP (1 μ M) and immunostained (4 DIV) for specific neuronal (Tuj-1) and axonal (Smi-312) markers. Arrowhead points to an axon turning at a baclofen stripe. Scale bar, 25 μ m. (h) Preferential index (defined in the text) for axon initiation on control F-BSA (5 μ g ml⁻¹), F-cAMP (20 μ M), baclofen or CGP stripes (3–4 independent experiments, \sim 300 cells per condition). In some experiments, forskolin (20 μ M) or SQ22536 (10 μ M) were bath applied to cultures. Asterisks: significant difference compared with controls (Kruskal-Wallis one-way ANOVA, $P = 0.016$; *post-hoc* Student-Newman-Keuls method, $P < 0.05$).

Statistical analysis. Statistical analysis was performed with Student's *t*-test or one-way ANOVA and *post-hoc* comparison. For datasets of non-normal distribution, Mann-Whitney rank sum test or Kruskal-Wallis one-way ANOVA on ranks test was used. All average data were presented as mean \pm s.e.m. The label 'Control' was used when a single example was reported in the figure, whereas 'Controls' was reported in summary graphs with averages. 'Controls' indicated that diverse types of controls were averaged (that is, cell transfected with empty vector, cells transfected with scramble siRNA, WT cells) after an appropriate statistical test established no differences among them.

References

- Ben-Ari, Y., Gaiarsa, J. L., Tyzio, R. & Khazipov, R. GABA: a pioneer transmitter that excites immature neurons and generates primitive oscillations. *Physiol. Rev.* **87**, 1215–1284 (2007).
- Wang, D. D. & Kriegstein, A. R. Defining the role of GABA in cortical development. *J. Physiol.* **587**, 1873–1879 (2009).
- Pinard, A., Seddik, R. & Bettler, B. GABAB receptors: physiological functions and mechanisms of diversity. *Adv. Pharmacol.* **58**, 231–255 (2010).
- Ben-Ari, Y. *et al.* Refuting the challenges of the developmental shift of polarity of GABA actions: GABA more exciting than ever! *Front. Cell. Neurosci.* **6** (2012).
- Fukuda, A., Mody, I. & Prince, D. A. Differential ontogenesis of presynaptic and postsynaptic GABAB inhibition in rat somatosensory cortex. *J. Neurophysiol.* **70**, 448–452 (1993).
- Owens, D. F. & Kriegstein, A. R. Is there more to GABA than synaptic inhibition? *Nat. Rev. Neurosci.* **3**, 715–727 (2002).
- Ben-Ari, Y. Excitatory actions of gaba during development: the nature of the nurture. *Nat. Rev. Neurosci.* **3**, 728–739 (2002).
- Lopez-Bendito, G. *et al.* Expression and distribution of metabotropic GABA receptor subtypes GABABR1 and GABABR2 during rat neocortical development. *Eur. J. Neurosci.* **15**, 1766–1778 (2002).
- Sernagor, E., Chabrol, F., Bony, G. & Cancedda, L. GABAergic control of neurite outgrowth and remodeling during development and adult neurogenesis: general rules and differences in diverse systems. *Front. Cell. Neurosci.* **4**, 11 (2010).
- Gaiarsa, J. L., Kuczewski, N. & Porcher, C. Contribution of metabotropic GABA(B) receptors to neuronal network construction. *Pharmacol. Ther.* **132**, 170–179 (2011).
- Priest, C. A. & Puche, A. C. GABAB receptor expression and function in olfactory receptor neuron axon growth. *J. Neurobiol.* **60**, 154–165 (2004).
- Xiang, Y. *et al.* Nerve growth cone guidance mediated by G protein-coupled receptors. *Nat. Neurosci.* **5**, 843–848 (2002).
- Maric, D. *et al.* GABA expression dominates neuronal lineage progression in the embryonic rat neocortex and facilitates neurite outgrowth via GABA(A) autoreceptor/Cl⁻ channels. *J. Neurosci.* **21**, 2343–2360 (2001).
- Behar, T. N. *et al.* GABA(B) receptors mediate motility signals for migrating embryonic cortical cells. *Cereb. Cortex* **11**, 744–753 (2001).
- Lopez-Bendito, G. *et al.* Blockade of GABA(B) receptors alters the tangential migration of cortical neurons. *Cereb. Cortex* **13**, 932–942 (2003).
- McClellan, K. M., Calver, A. R. & Tobet, S. A. GABAB receptors role in cell migration and positioning within the ventromedial nucleus of the hypothalamus. *Neuroscience* **151**, 1119–1131 (2008).
- Behar, T. N., Schaffner, A. E., Scott, C. A., Greene, C. L. & Barker, J. L. GABA receptor antagonists modulate postmitotic cell migration in slice cultures of embryonic rat cortex. *Cereb. Cortex* **10**, 899–909 (2000).
- Haller, C. *et al.* Floxed allele for conditional inactivation of the GABAB(1) gene. *Genesis* **40**, 125–130 (2004).
- Schuler, V. *et al.* Epilepsy, hyperalgesia, impaired memory, and loss of pre- and postsynaptic GABA(B) responses in mice lacking GABA(B1). *Neuron* **31**, 47–58 (2001).
- Thuault, S. J. *et al.* Mechanisms contributing to the exacerbated epileptiform activity in hippocampal slices expressing a C-terminal truncated GABA(B2) receptor subunit. *Epilepsy Res.* **65**, 41–51 (2005).
- Vigot, R. *et al.* Differential compartmentalization and distinct functions of GABAB receptor variants. *Neuron* **50**, 589–601 (2006).
- Gassmann, M. *et al.* Redistribution of GABAB(1) protein and atypical GABAB responses in GABAB(2)-deficient mice. *J. Neurosci.* **24**, 6086–6097 (2004).
- Queva, C. *et al.* Effects of GABA agonists on body temperature regulation in GABA(B1) $-/-$ mice. *Br. J. Pharmacol.* **140**, 315–322 (2003).
- Fiorantino, H. *et al.* GABA(B) receptor activation triggers BDNF release and promotes the maturation of GABAergic synapses. *J. Neurosci.* **29**, 11650–11661 (2009).
- Wu, Y. *et al.* Transgenic mice over-expressing GABA(B)R1a receptors acquire an atypical absence epilepsy-like phenotype. *Neurobiol. Dis.* **26**, 439–451 (2007).
- Stewart, L. S. *et al.* Severity of atypical absence phenotype in GABAB transgenic mice is subunit specific. *Epilepsy Behav.* **14**, 577–581 (2009).
- Kriegstein, A. R. Constructing circuits: neurogenesis and migration in the developing neocortex. *Epilepsia* **46**(Suppl 7) 15–21 (2005).
- Saito, T. & Nakatsuji, N. Efficient gene transfer into the embryonic mouse brain using *in vivo* electroporation. *Dev. Biol.* **240**, 237–246 (2001).
- Cancedda, L., Fiumelli, H., Chen, K. & Poo, M. M. Excitatory GABA action is essential for morphological maturation of cortical neurons *in vivo*. *J. Neurosci.* **27**, 5224–5235 (2007).
- Barnes, A. P. & Polleux, F. Establishment of axon-dendrite polarity in developing neurons. *Annu. Rev. Neurosci.* **32**, 347–381 (2009).
- Dal Maschio, M. *et al.* High-performance and site-directed in utero electroporation by a triple-electrode probe. *Nat. Commun.* **3**, 960 (2012).
- Martin, S. C. *et al.* Differential expression of gamma-aminobutyric acid type B receptor subunit mRNAs in the developing nervous system and receptor coupling to adenylyl cyclase in embryonic neurons. *J. Comp. Neurol.* **473**, 16–29 (2004).
- Cheng, P. L. & Poo, M. M. Early events in axon/dendrite polarization. *Annu. Rev. Neurosci.* **35**, 181–201 (2012).
- Shelly, M., Cancedda, L., Heilshorn, S., Sumbre, G. & Poo, M. M. LKB1/STRAD promotes axon initiation during neuronal polarization. *Cell* **129**, 565–577 (2007).
- Shelly, M. *et al.* Local and long-range reciprocal regulation of cAMP and cGMP in axon/dendrite formation. *Science* **327**, 547–552 (2010).
- Shelly, M. *et al.* Semaphorin3A regulates neuronal polarization by suppressing axon formation and promoting dendrite growth. *Neuron* **71**, 433–446 (2011).
- Barnes, A. P. *et al.* LKB1 and SAD kinases define a pathway required for the polarization of cortical neurons. *Cell* **129**, 549–563 (2007).
- Yi, J. J., Barnes, A. P., Hand, R., Polleux, F. & Ehlers, M. D. TGF-beta signaling specifies axons during brain development. *Cell* **142**, 144–157 (2010).
- Engelhardt, B. Development of the blood-brain barrier. *Cell Tissue Res.* **314**, 119–129 (2003).
- Demarque, M. *et al.* Paracrine intercellular communication by a Ca2+ - and SNARE-independent release of GABA and glutamate prior to synapse formation. *Neuron* **36**, 1051–1061 (2002).
- Prosser, H. M. *et al.* Epileptogenesis and enhanced prepulse inhibition in GABA(B1)-deficient mice. *Mol. Cell Neurosci.* **17**, 1059–1070 (2001).
- Signorini, S., Liao, Y. J., Duncan, S. A., Jan, L. Y. & Stoffel, M. Normal cerebellar development but susceptibility to seizures in mice lacking G protein-coupled, inwardly rectifying K+ channel GIRK2. *Proc. Natl Acad. Sci. USA* **94**, 923–927 (1997).
- Eisenberg, B. & Messer, A. Tonic/clonic seizures in a mouse mutant carrying the weaver gene. *Neurosci. Lett.* **96**, 168–172 (1989).
- Brown, J. T. *et al.* Mechanisms contributing to the exacerbated epileptiform activity in hippocampal slices of GABAB1 receptor subunit knockout mice. *Epilepsy Res.* **57**, 121–136 (2003).
- Calderon de Anda, F., Gartner, A., Tsai, L. H. & Dotti, C. G. Pyramidal neuron polarity axis is defined at the bipolar stage. *J. Cell Sci.* **121**, 178–185 (2008).
- Wu, Q. F. *et al.* Fibroblast growth factor 13 is a microtubule-stabilizing protein regulating neuronal polarization and migration. *Cell* **149**, 1549–1564 (2012).
- Cheng, P. L., Lu, H., Shelly, M., Gao, H. & Poo, M. M. Phosphorylation of e3 ligase smurf1 switches its substrate preference in support of axon development. *Neuron* **69**, 231–243 (2011).
- Nakamura, S. *et al.* Local application of neurotrophins specifies axons through inositol 1,4,5-trisphosphate, calcium, and Ca2+ /calmodulin-dependent protein kinases. *Sci. Signal* **4**, ra76 (2011).
- Nagano, T., Morikubo, S. & Sato, M. Filamin A and FILIP (filamin A-interacting protein) regulate cell polarity and motility in neocortical subventricular and intermediate zones during radial migration. *J. Neurosci.* **24**, 9648–9657 (2004).
- Filip, M. & Frankowska, M. GABA(B) receptors in drug addiction. *Pharmacol. Rep.* **60**, 755–770 (2008).
- Zhang, J. *et al.* Brefeldin A-inhibited guanine exchange factor 2 regulates filamin A phosphorylation and neuronal migration. *J. Neurosci.* **32**, 12619–12629 (2012).
- Meijering, E. *et al.* Design and validation of a tool for neurite tracing and analysis in fluorescence microscopy images. *Cytometry A* **58**, 167–176 (2004).

Acknowledgements

We thank M. Canossa, IIT Genoa, Italy, for providing mGFP, F-cAMP, F-BSA; L. Berdondini, IIT, Genoa, Italy, for generating the template of the stripe moulds; and Dr K. Kaupmann, Novartis, Basel, Switzerland, for providing GABA_{B1a}, GABA_{B1b} and GABA_{B2}. We are grateful to the members of IIT molecular biology, cell culture, imaging and animal facilities, and to Dr A. Diaspro's laboratory for technical support. The work was supported by Compagnia di San Paolo grant no. 2008.1267.

Author contributions

G.B. Performed IUE, immunohistochemistry, image acquisition, electrophysiological recordings, data analysis, wrote part of the manuscript and realized the figures. J.S. participated in IUE, performed immunostaining and realized part of the figures. I.T. performed biochemistry experiments. M.S. provided the LKB1 and LKB1-siRNA vectors, and prepared LKB1-S431E. A.C. constructed GABA_B vectors, screened shRNAi, prepared

cell cultures and performed biochemistry experiments. L.C. performed part of data analysis and image acquisition, designed the experiments and wrote the manuscript. All authors revised the manuscript.

Additional information

Supplementary Information accompanies this paper at <http://www.nature.com/naturecommunications>

Competing financial interests: The authors declare no competing financial interests.

Reprints and permission information is available online at <http://npg.nature.com/reprintsandpermissions/>

How to cite this article: Bony, G. *et al.* Non-hyperpolarizing GABA_B receptor activation regulates neuronal migration and neurite growth and specification by cAMP/LKB1. *Nat. Commun.* 4:1800 doi: 10.1038/ncomms2820 (2013).